

Japan's Efforts to Develop the Concept of JA DEMO During the Past Decade

Kenji Tobita, Ryoji Hiwatari, Yoshiteru Sakamoto, Youji Someya, Nobuyuki Asakura, Hiroyasu Utoh, Yuya Miyoshi, Shinsuke Tokunaga, Yuki Homma, Satoshi Kakudate, Noriyoshi Nakajima & the Joint Special Design Team for Fusion DEMO

To cite this article: Kenji Tobita, Ryoji Hiwatari, Yoshiteru Sakamoto, Youji Someya, Nobuyuki Asakura, Hiroyasu Utoh, Yuya Miyoshi, Shinsuke Tokunaga, Yuki Homma, Satoshi Kakudate, Noriyoshi Nakajima & the Joint Special Design Team for Fusion DEMO (2019) Japan's Efforts to Develop the Concept of JA DEMO During the Past Decade, Fusion Science and Technology, 75:5, 372-383, DOI: [10.1080/15361055.2019.1600931](https://doi.org/10.1080/15361055.2019.1600931)

To link to this article: <https://doi.org/10.1080/15361055.2019.1600931>



© 2019 The Author(s). Published with license by Taylor & Francis Group, LLC.



Published online: 07 May 2019.



Submit your article to this journal [↗](#)



Article views: 116



View Crossmark data [↗](#)



Japan's Efforts to Develop the Concept of JA DEMO During the Past Decade

Kenji Tobita,^{*a} Ryoji Hiwatari,^a Yoshiteru Sakamoto,^a Youji Someya,^a Nobuyuki Asakura,^a Hiroyasu Utoh,^a Yuya Miyoshi,^a Shinsuke Tokunaga,^a Yuki Homma,^a Satoshi Kakudate,^a Noriyoshi Nakajima,^b and the Joint Special Design Team for Fusion DEMO^a

^aNational Institutes for Quantum and Radiological Science and Technology, Rokkasho, Aomori 039-3212, Japan

^bNational Institute for Fusion Science, Rokkasho, Aomori 039-3212, Japan

Received June 15, 2018

Accepted for Publication March 26, 2019

Abstract — This paper summarizes the evolution of Japanese DEMO design studies in a retrospective manner by highlighting efforts to resolve critical design issues on DEMO. Japan is currently working on the conceptual study of a steady-state DEMO (JA DEMO) with a major radius R_p of 8.5 m and fusion power P_{fus} of 1.5 to 2 GW based on water-cooled solid breeding blanket with pressurized water reactor water condition (290°C to 325°C, 15.5 MPa). Such a lower P_{fus} allows to find realistic design solutions for divertor heat removal. Recognizing that divertor heat removal is one of the most challenging issues on DEMO, the divertor design has been carried out in different approaches, including numerical divertor plasma simulation, magnetic configurations, heat sink design, etc. It is noteworthy that the latest divertor simulation led to a design window allowing divertor heat removal of the peak heat flux of $<10 \text{ MW/m}^2$. The breeding blanket (BB) design has been concentrated on simplification of the internal structure and pressure tightness of the BB casing against the in-box loss-of-coolant accident. Due to a large amount of radioactive waste generated in periodic replacement of in-vessel components, downsizing of waste-related facilities has come to be regarded as a significant design issue. A possible waste management for reducing temporary waste storage was proposed, and its impact on the plant layout was assessed.

Keywords — DEMO, fusion reactor, diverter, blanket, radioactive waste.

Note — Some figures may be in color only in the electronic version.

I. INTRODUCTION

In parallel with the steady progress of ITER construction, many countries express increasing interest in post-ITER programs toward the realization of fusion power.^{1–6} Since the middle of the 2000s, Japanese

reactor studies have been devoted to DEMO conceptual designs, and dozens of papers dealing with the conceptual designs have been published so far. Most of them deal with progress and updates of specific design issues, and thus it is perhaps hard to know an overall history of the design philosophy from the published literature. The purpose of this paper is to summarize the Japanese DEMO (JA DEMO) design studies during the past decade in a retrospective manner and to characterize Japan's efforts to address DEMO design challenges aimed at design consistency and feasibility.

Japan is currently working on the design activity of a steady-state JA DEMO with a major radius R_p of 8.5 m and fusion power P_{fus} of 1.5 to 2 GW based on

*E-mail: tobita.kenji@qst.go.jp

This is an Open Access article distributed under the terms of the Creative Commons Attribution-NonCommercial-NoDerivatives License (<http://creativecommons.org/licenses/by-nc-nd/4.0/>), which permits non-commercial re-use, distribution, and reproduction in any medium, provided the original work is properly cited, and is not altered, transformed, or built upon in any way.

a water-cooled solid breeding (WCSB) operated under the same water condition as pressurized water reactors (290°C to 325°C, 15.5 MPa). The design could be considered as a significant compromise with conservative design parameters, especially regarding P_{fus} and a normalized beta β_N when compared with previous DEMO concepts such as SlimCS (Refs. 7 and 8) and Demo-CREST (Refs. 9 and 10). SlimCS was designed to produce $P_{fus} = 2.95$ GW at $R_p = 5.5$ m assuming WCSB with subcritical water condition (290°C to 360°C, 23 MPa), while Demo-CREST eventually aims to attain $P_{fus} = 3$ GW and $\beta_N > 4$ at $R_p = 7.3$ m. The update of the requirements for DEMO in 2015 is responsible for the change from compact DEMOs producing high fusion power ($P_{fus} \sim 3$ GW) to JA DEMO with a lower P_{fus} and larger R_p .

In this paper, the background of the change in design philosophy is described in Sec. II. In Sec. III, a brief overview of the current JA DEMO is presented. The latest results of the JA DEMO design are presented together with design updates and changes during the past decade in Sec. IV.

II. DEMO DEVELOPMENT STRATEGY

Before 2015, DEMO was required to satisfy (1) a reactor size similar to that of ITER, (2) the electricity generation capability of a gigawatt level, (3) steady-state operation, and (4) tritium breeding meeting self-sufficient production of fuel in closed cycle, along with the report by the Advisory Committee on Nuclear Fusion under the Atomic Energy Commission of Japan.¹¹ Under the requirements, previous DEMO conceptual studies such as SlimCS and Demo-CREST focused on a compact DEMO producing a fusion power of 3 GW being equivalent to

electricity of 1 GW. Hence, the lesson learned from these DEMO studies is the difficulty in handling such a high power with existing or foreseeable technology, especially in divertor heat removal. This problem had an impact on the arguments about the goals of DEMO among the Japanese fusion community in the 2010s, and thus the target on the output has been updated to “steady and stable power generation beyond several hundreds of MW” (Ref. 12). Such a change in the development policy created the circumstances to explore a DEMO concept with a larger R_p and lower P_{fus} . In the same year, the DEMO design activities in Japan were unified to a single team called the Joint Special Design Team for Fusion DEMO (Ref. 13). The evolution of the DEMO designs is summarized in Fig. 1. In alignment with the updated requirements, “A Roadmap for Fusion DEMO Reactor” was formulated by the Science and Technology Committee on Fusion Energy under the Ministry of Education, Culture, Sports, Science and Technology in 2018 (Ref. 14).

III. JAPANESE DEMO

Since the original concept of the JA DEMO was defined in 2014 (Ref. 15), the pre-conceptual design has been continued on the DEMO reactor and balance of plant. Based on Refs. 11 and 14, the DEMO is requested to be a steady-state tokamak with WCSB blanket. Figure 2 is a cut-away view of the JA DEMO. The DEMO is characterized with a somewhat large major radius R_p of 8.5 m for volt-second supply for operational flexibility, and low fusion power P_{fus} of 1.5 to 2 GW for divertor heat removal. The main design parameters of the JA DEMO for $P_{fus} = 1.42$ GW are listed in Table I. The thermal power extracted from the DEMO as pressurized water of ~300°C is 1879 MW (Ref. 13), with the

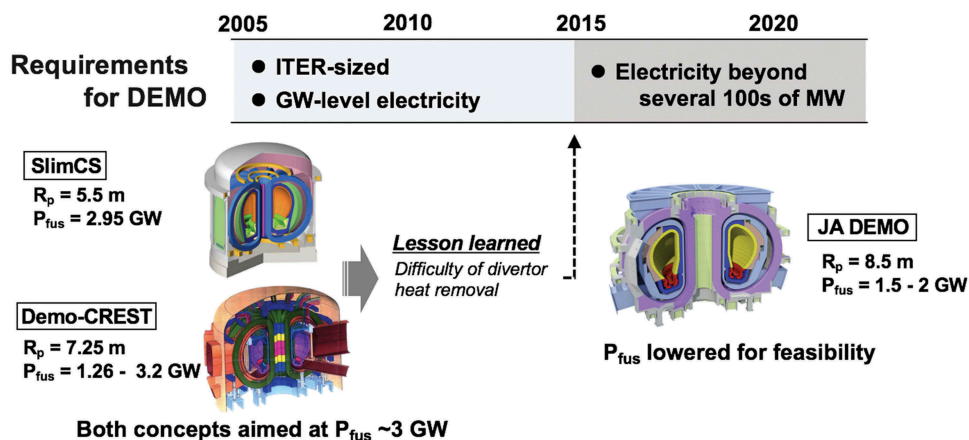


Fig. 1. Evolution of DEMO designs in Japan.

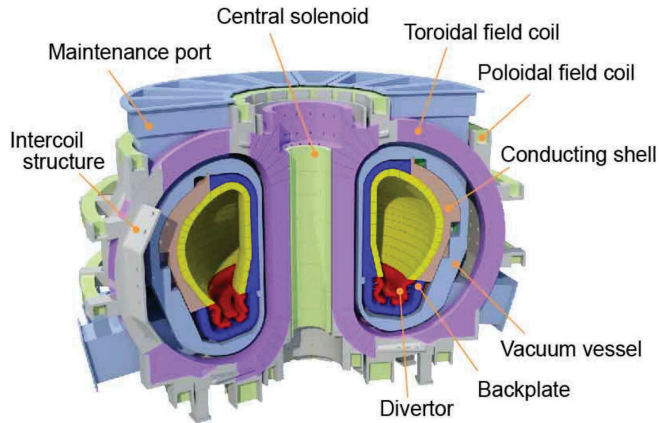


Fig. 2. Conceptual view of the JA DEMO.

consideration of energy multiplication in the in-vessel components (IVCs) being anticipated to generate about 630 MW of gross electricity.¹⁶ The preliminary estimate indicates the net electricity production exceeding 300 MW. The central solenoid provides a poloidal flux (volt-second) of more than 400 Wb by bipolar flux swing, allowing electric power generation in power-up phase planned in early deuterium-tritium operation albeit pulsed and low power. Due to the relatively low P_{fus} design, the required plasma electron density n_e is as low as $n_e = 0.66 \times 10^{20} \text{ m}^{-3}$, which is the same as that in ITER. An important question on such a low n_e design is whether or not plasma detachment is possible. The divertor simulation in Sec. IV indicates a feasibility of plasma detachment and divertor heat removal in the design parameters. The average neutron wall load (NWL) is 1 MW/m^2 , and the peak NWL reaches 1.5 MW/m^2 on the outer midplane. The average NWL in the divertor region is as low as 0.3 MW/m^2 . Table II summarizes the design changes of DEMOs during the past decade.

The timeline of DEMO development is as follows:

1. pre-conceptual design phase (up to around 2020)

2. conceptual design phase (around 2020 to 2025)
3. engineering design phase (around 2025 to 2035).

Since the DEMO development program is defined on the premise of the success of ITER, the key years of the program in the timeline will be subject to change in accordance with the progress of ITER. The current DEMO design is in the pre-conceptual design phase in which the fundamental concept of DEMO with design consistency is developed and the research and development needs for DEMO are defined to start large- or plant-scale development toward DEMO construction.

IV. DIVERTOR DESIGN

IV.A. Overview of Divertor Design

The current baseline design of the divertor is based on (1) conventional single null divertor (SND) with a divertor leg longer than ITER (1 m in the poloidal projection length on ITER), (2) plasma detachment with impurity seeding, and (3) ITER-like tungsten monoblock heat sink cooled by pressurized water. Before reaching the baseline, various approaches have been carried out as depicted in Fig. 3, including the assessment of different divertor configurations, divertor simulation, heat sink design, and the consideration of remote maintenance (RM).

The assessment of divertor configurations encompassed (1) conventional SND with different divertor legs, and (2) advanced divertor configurations such as “super-X” (SXD) and “snowflake” (SFD). The former approach is to facilitate plasma detachment by extending the connection length of magnetic field lines in the divertor, and the latter is to stretch the flux tubes of the divertor leg and to reduce the heat flux on the divertor target plate. Regarding divertor heat sink, the liquid divertor is excluded from the divertor heat sink option.

TABLE I

Design Parameters of the JA DEMO

Major radius, R_p (m)	8.5	Current drive power, P_{CD} (MW)	83.7
Minor radius, a (m)	2.42	Fusion gain, Q	17.5
Aspect ratio, A	3.5	Electron density, n_e (10^{20} m^{-3})	0.66
Plasma elongation, κ_{95}	1.65	Normalized density, n_e/n_{GW}	1.2
Safety factor, q_{95}	4.1	Ave. electron temp., $\langle T_e \rangle$ (keV)	16.0
Plasma current, I_p (MA)	12.3	Confinement enhancement, HHy2	1.31
Magnetic field on axis, B_T (T)	5.94	Normalized beta, β_N	3.4
Maximum field, B_{max} (T)	13.7	Bootstrap fraction, f_{BS}	0.61
Fusion power, P_{fus} (GW)	1.42	Average wall load, NWL (MW/m^2)	1.0

TABLE II
Design Changes During the Past Decade

	Previous DEMOs (~2010)	Current DEMO (2018)
	SlimCS/Demo-CREST	JA DEMO
Plasma major radius	5.5 to 7.25 m	8.5 m
Fusion output	~3 GW	1.5 to 2 GW
SC magnet (TF coils)	Nb ₃ Al ($B_{max} \sim 16$ T)	Nb ₃ Sn ($B_{max} \sim 13$ T)
Remote maintenance	Sector or large module transport using large ports	Banana segment and divertor cassette transport using small port
Breeding blanket	In-box LOCA not considered; layered packing of Li ₄ SiO ₄ , Be and Be ₁₂ Ti pebbles	In-box LOCA considered; full mixture packing of Li ₂ TiO ₃ and Be ₁₂ V (Be ₁₃ Zr) pebbles
Divertor	Single null; detachment; water cooled W-monoblock; RAFM cooling pipe	Same as before; RAFM/Cu-alloy pipes

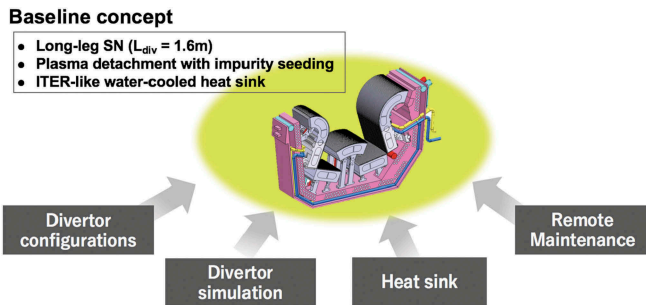


Fig. 3. Approaches to define the baseline divertor concept.

Thus, a solid divertor target based on an extension of ITER-like tungsten monoblock heat sink is considered to be the only candidate for JA DEMO in light of engineering maturity.

A prime design issue on the divertor is to pursue a solution for divertor heat removal under these constraints, namely SND with the ITER-like tungsten monoblock heat sink. When the heat sink is a combination of CuCrZr cooling pipes and low temperature water of about 200°C, the allowable heat flux of the heat sink is 10 MW/m² or lower. Accordingly, the peak heat flux on the divertor target q_{div}^{peak} of 10 MW/m² or lower for $P_{fus} = 1.5$ to 2 GW can be a solution for divertor heat removal. The basic concept of divertor heat removal is power dissipation by seeding impurity. Radiation due to Bremsstrahlung, synchrotron, and line radiation from the core plasma

dissipates about 40% of the absorbed power of the core plasma. Another 40% is dissipated in the scrape-off-layer (SOL) and divertor (as a result, the total radiation amounts to 80%), and eventually the remaining power of 20% reaches the divertor, satisfying $q_{div}^{peak} \leq 10$ MW/m². In order to find solutions supporting the divertor concept, numerical simulations with a SONIC code have been carried out for more than a decade as described in Sec. IV.D. It is remarkable that the situation of the simulations has made progress so as to discuss a design window for divertor heat removal that is more valuable than a few design points.

IV.B. Divertor Configurations

Divertor geometry plays a determinant role in reducing divertor heat flux. Different divertor configurations illustrated in Fig. 4 were assessed for JA DEMO:

1. *Conventional SND*: A W-shaped SND with vertical target plates adopted in ITER is efficient to enhance particle recycling near the strike points and produce detached plasma. In the JA DEMO that handles 1.5 to 2 GW, which is three or four times higher power than ITER, the long divertor leg L_{div} of 1.6 to 2 m (ITER ~ 1 m) in Fig. 4a was considered to facilitate plasma detachment due to an extension of the divertor connection length. As a result of divertor simulation, it is concluded that the SND with even shorter $L_{div} = 1.6$ m, albeit longer than that of

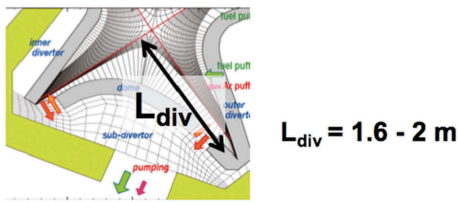
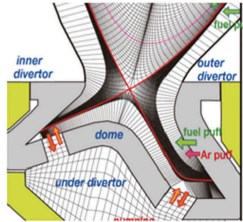
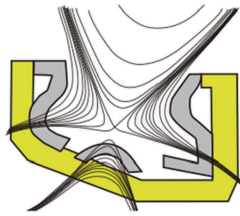
(a) Conventional Single Null Div (SND)**(b) Super X div (SXD)****(c) Snowflake div (SFD)**

Fig. 4. Divertor configurations considered for divertor heat removal on the JA DEMO. (a) The conventional single null divertor is selected as the baseline design from various aspects of assessment.

ITER, can handle $P_{fus} = 1.5$ to 2 GW (Ref. 17) and is selected as the baseline of the divertor configuration.

2. *Advanced divertor configurations:* Another approach for reducing the divertor heat load is a flux tube expansion in the divertor with SXD or SFD configuration as shown in Figs. 4b and 4c. An engineering challenge in such configurations is a high magnetic field required for modifying the field lines in the divertor region. A magnetohydrodynamic equilibrium analysis for JA DEMO indicates that high poloidal currents exceeding 100 MegaAmpere-turns (MAT) are required when the poloidal field (PF) coils are arranged like conventional tokamak reactors. Assuming that a square superconductor of 0.04×0.04 m has a current density of 40 to 50 kA, the cross section of the PF coil equivalent to 100 MAT becomes as large as 4 m^2 . The problem could be resolved by means of inter-link winding in which parts of PF coils are arranged near the divertor inside the toroidal field (TF) coil bore to reduce the required ampere-turns.¹⁸ Nevertheless, considerations on engineering feasibility concluded the technology is too premature to adopt as a possible divertor option. This is because the inter-link winding has difficulties in in-situ winding, the low alternating-current loss superconductor which is operative under high field, and the assembly process of TF coils, inter-linked PF coils and the vacuum vessel (VV).¹⁹ The divertor simulation for SXD shows that a significant radiation region is produced between the super-X null (second null point) and the divertor target, and that the radiation loss in the divertor increases, producing fully detached plasma

efficiently.¹⁷ However, the resulting heat load to the divertor is critical in light of an engineering constraint in that a concentration of radiated power reaches 10 MW/m^2 on the divertor target plate.

IV.C. Divertor Cassette Design

Divertor heat sink is designed to remove thermal load with W-armored Cu alloy (CuCrZr) pipe ($\sim 200^\circ\text{C}$ cooling water) near the strike points and reduce activation ferritic/martensitic (RAFM) steel pipe ($\sim 300^\circ\text{C}$ cooling water) in the other parts.²⁰ The design window on the operating temperature of the Cu alloy and RAFM steel is set in the range of 200°C to 350°C and 280°C to 550°C , respectively, considering the limits of material strength and ductility under the neutron irradiation environment. Radiation damage [displacements per atom (dpa)] of the Cu alloy and RAFM pipe is estimated to be in the range of 0.3 to 2.3 and 1.5 to 6.7 dpa, respectively, for a full-power-year (FPY) operation of the DEMO at $P_{fus} = 1.5$ GW. The water condition for the Cu alloy pipe is 200°C , 5 MPa, and 9.7 m/s in the inlet and 231°C in the outlet, and the coolant condition for the RAFM pipe is 250°C , 15 MPa, and about 4 m/s in the inlet and 325°C in the outlet. The water condition was determined to satisfy divertor heat removal and the operating temperature window of the pipe materials.

The VV should be made of stainless steel from the aspect of fabrication in that stainless steel has an advantage in thick welding required for the fabrication of the VV. In addition, from the aspect that the VV is a safety class component, which works as the first barrier, it is reasonable to fabricate the VV with stainless steel-based proven technology. Stainless steel needs to be used in the environment where helium embrittlement due to neutron irradiation is avoided. For this purpose, the divertor cassette is required to have a function of softening neutron spectrum much lower than 1 MeV. The problem of previous divertor cassette design was to satisfy such neutron shielding without impairing vacuum pumping capability. The updated design for the divertor cassette is depicted in Fig. 5. The outer frame of the cassette is made of 0.2-m-thick RAFM steel with water cooling channel. The pumping slot of the cassette is a labyrinthine structure to meet a neutron irradiation of lower than 0.1 dpa/FPY on the inner VV surface.

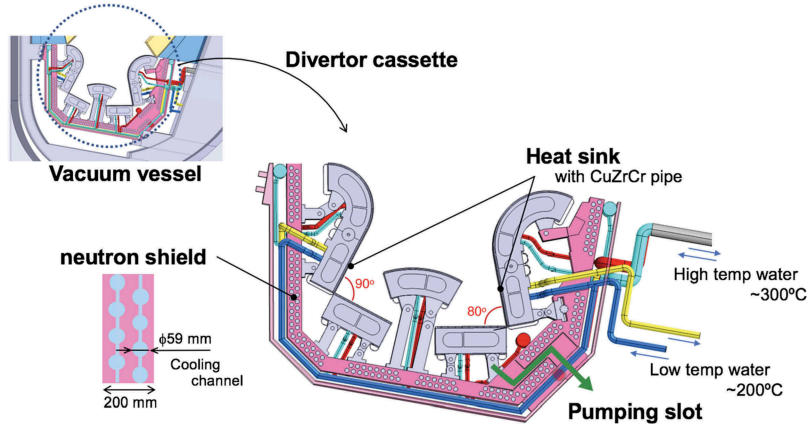


Fig. 5. Conceptual design of divertor cassette.

IV.D. Divertor Simulation Study

Numerical simulation is necessary to predict the behavior of divertor plasma and to find probable operation condition for divertor heat removal on DEMO. For the application to DEMO, a SONIC code^{21–24} has been developed so as to treat multiple impurities seeding for plasma detachment in different divertor geometries. Previous interest in the early divertor simulation with the SONIC code was to find a solution for satisfying $q_{div}^{peak} < 10 \text{ MW/m}^2$. Since then, a lot of solutions have been obtained, and thus our interest moves on to the design or operation window for allowing divertor heat removal.

The simulation result of a parameter scan is shown in Fig. 6, where the power inflow to the SOL, P_{sep} , and impurity (Ar) seed condition are changed for the baseline divertor design.²⁵ Here, P_{sep} is given by $P_{sep} = P_{in} (1 - f_{rad}^{main})$ with the input power to the main plasma P_{in} and the radiation loss fraction in the main plasma f_{rad}^{main} . Roughly speaking, $P_{sep} \sim 250 \text{ MW}$ and $P_{sep} \sim 300 \text{ MW}$ correspond to $P_{fus} \sim 1.5 \text{ GW}$ and $P_{fus} \sim 2 \text{ GW}$, respectively. In the case of the total radiation f_{rad} of $\sim 80\%$, the design window satisfying $q_{div}^{peak} < 10 \text{ MW/m}^2$ is seen at the separatrix density n_{sep} of about $2 \times 10^{19} \text{ m}^{-3}$ or higher even for $P_{sep} \sim 300 \text{ MW}$ as well as $P_{sep} \sim 250 \text{ MW}$. The design window of n_{sep} is reasonable in terms of plasma operation in that n_{sep} is about one-third of n_e . In the region, the impurity content n_{Ar}/n_e is lower than 1% in the SOL. In contrast, in the case of $f_{rad} \sim 70\%$, the design window upshifts to $n_{sep} \geq 2.4 \times 10^{19} \text{ m}^{-3}$, which is unlikely as an operation region because of high n_{sep}/n_e . It is concluded from the simulation that the design target for divertor heat removal with Ar seeding is $f_{rad} \sim 80\%$ and $n_{sep} \sim 2 \times 10^{19} \text{ m}^{-3}$ or higher for the JA DEMO.

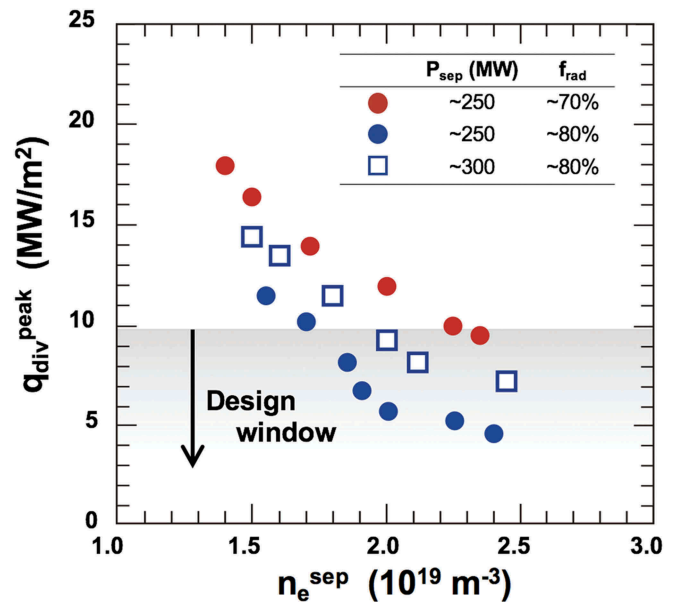


Fig. 6. Divertor simulation for the baseline design. P_{sep} and f_{rad} represent the power inflow to the SOL and the total radiation fraction, respectively.

V. BREEDING BLANKET

Since 2010, major and minor design updates on the breeding blanket (BB) have been made several times. The major updates are illustrated in Fig. 7. The initial BB concept for SlimCS (Fig. 7a) (Ref. 26) is a variation of WCSB with supercritical water.²⁷ The major problem of the concept is the complexity of the BB interior. Figure 7b is a BB concept aimed at simplifying the internal structure and adopting a full mixture of neutron multiplier (Be_{12}Ti) and tritium breeder (Li_2TiO_3) pebbles.²⁸ As the prime candidate for breeding material, Li_2TiO_3 was selected due to its good tritium release characteristic. Such a full mixture of Be_{12}Ti and Li_2TiO_3 pebbles benefits the tritium

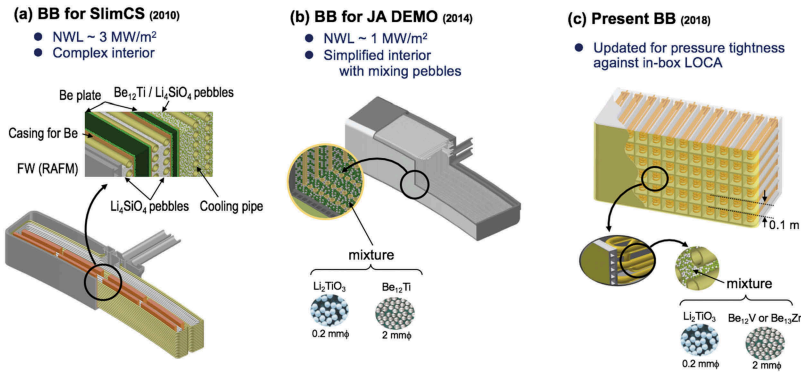


Fig. 7. Evolution of BB concept.

breeding ratio (TBR) compared with a separated arrangement of these pebbles with RAFM partitions. The mixture ratio of the pebbles was determined to be $\text{Be}_{12}\text{Ti}:\text{Li}_2\text{TiO}_3 = 7:3$ for the most efficient tritium production.

The current design study is concentrated on the BB structure to withstand the inner pressure load due to a break of cooling pipe inside the BB in case of an “in-box” loss-of-coolant accident (LOCA) due to a break of cooling pipe.²⁹ In order to withstand an inner pressure of 17.2 MPa due to an in-box LOCA, the BB module needs to be divided into 0.1×0.1 -m-wide cells with 0.015-m-thick ribs as seen in Fig. 7c. The main specifications of the BB concept are listed in Table III. In the design, the neutron multiplier is replaced by Be_{12}V or Be_{13}Zr because of advantages in the fabrication process and chemical stability. The previous design adopted beryllide pebbles (Be_{12}Ti) granulated with discharge between

a tungsten electrode and a rotating beryllide one.³⁰ The problem of Be_{12}Ti was that the compositional structure changes by peritectic reaction during cooling and the fact that the pebbles contain $\text{Be}_{17}\text{Ti}_2$ of 55% and Be of 11%. Such inhomogeneous composition is resolved by vacuum annealing, producing Be_{12}Ti single-phase.³¹ In contrast, Be_{12}V and Be_{13}Zr do not require homogenization treatment. In addition, Be_{12}V and Be_{13}Zr have more excellent oxidation resistance than Be_{12}Ti and show lower H_2 generation with water vapor,^{32,33} which is advantageous in terms of safety.

The problem of the BB concept with rib structure is a reduction in the volume fraction of breeder, being only 68% for the case of Fig. 7c. The anticipated TBR is as low as 1.02. In order to overcome the problem, a honeycomb-shaped rib structure (Fig. 8) is presently under study.²⁵ The fraction of breeder volume increases up to 77% in this design and the resulting TBR is estimated to be 1.07. The fabrication of these rib structures is based on the premise of the development of reliable hot isostatic pressing and its inspection technology on joint surfaces. Continuing efforts are being made to attain higher TBR by maximizing BB coverage and BB thickness or replacing the coolant from light water to heavy water.

TABLE III

Main Specifications of the Current BB Design

Structural material	RAFM (F82H)
Coolant	Pressurized water (290°C to 325°C), 15.5 MPa
Neutron multiplier	Be_{12}V or Be_{13}Zr pebbles (2 mm in diameter)
Tritium breeder	Li_2TiO_3 (0.2 mm in diameter), 90% enrichment of ^6Li
Packing	Full mixture of Be_{12}V (70%) and Li_2TiO_3 pebbles (30%)
Dimension of BB casing	Typically, 1.44 m (width) \times 0.73 m (height) \times 0.6 m (depth)
Rib	15 mm thick, with water cooling channels (7%)

VI. SUPERCONDUCTING MAGNETS

Since DEMO requires a high field exceeding 13 T and larger plasma volume than ITER, the magnetic energy of the TF coils becomes tremendously large. Considering the high field and stress acting in the coils, Nb_3Al was originally the prime conductor option due to a high operation current in high field and less susceptibility of the operation current to a strain. Actually, SlimCS and Demo-CREST adopted the Nb_3Al conductor for TF coils to attain the maximum field of about 16 T. Hence, throughout the

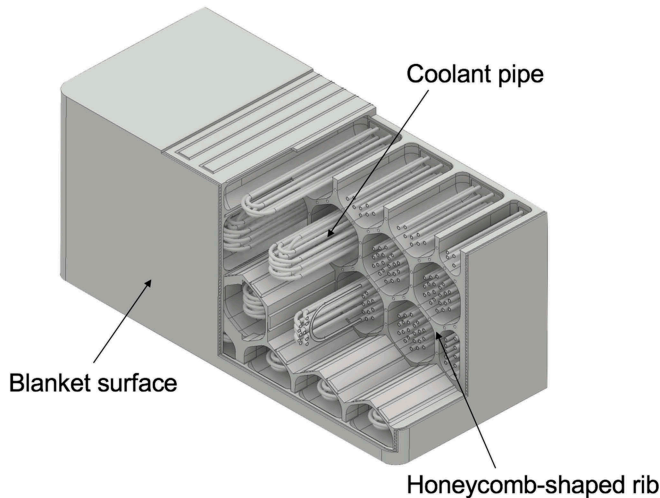


Fig. 8. Ongoing BB design with honeycomb-shaped rib structure.

design study of the JA DEMO with a TF coil design code named SCONE (Ref. 34), it was found that, for a larger R_p ($\geq 8\text{m}$) design, the attainable B_{max} is limited to $\sim 13\text{ T}$ and that an advantage for reaching higher B_{max} is dramatically reduced as shown in Fig. 9. In Fig. 9, it should also be noted that the design stress S_m has a large impact on the high field TF coil design and that an increase of S_m from 670 MPa (used in ITER) to 800 MPa leads to a B_{max} increment of 1 T. Based on the result, the JA DEMO adopted $S_m = 800\text{ MPa}$.

Figure 10 illustrates the plasma cross section and TF coils of DEMO and ITER. A comparison of the design parameters of the TF coils between DEMO and ITER is given in Table IV. Considering the high field

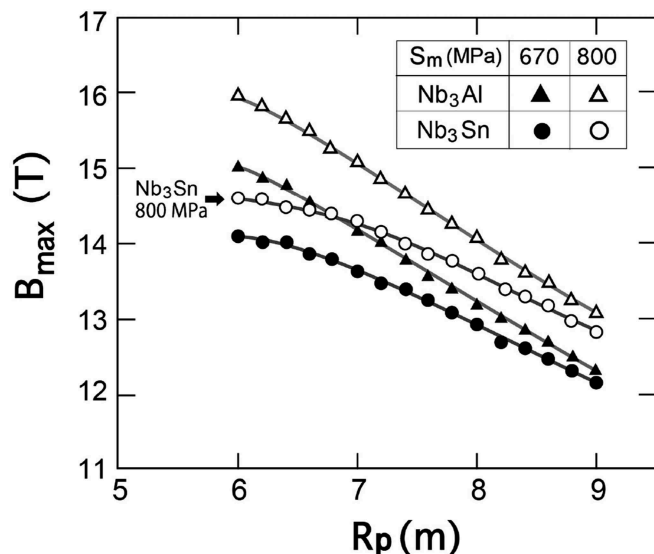


Fig. 9. B_{max} for Nb_3Sn and Nb_3Al as a function of R_p .

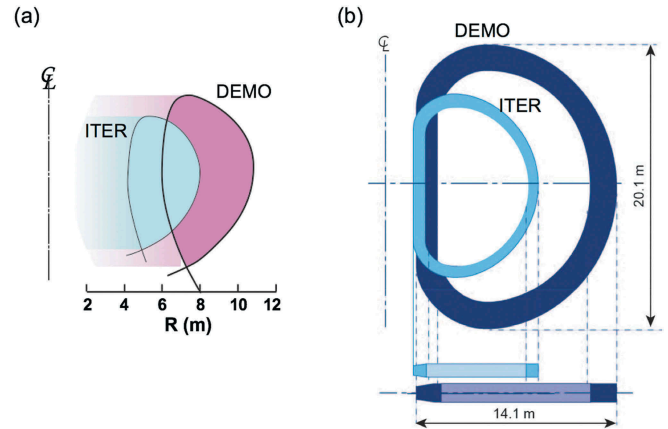


Fig. 10. Comparison of (a) plasma size and (b) TF coil size between DEMO and ITER.

TABLE IV

Comparison of TF Coils Between the JA DEMO and ITER

	JA DEMO	ITER
Conductor	Nb_3Sn	Nb_3Sn
Number of TF coils	16	18
Maximum field	13.7 T	11.8 T
Total magnetic energy	149 GJ	41 GJ
MAT in all TF coils	255 MAT	164 MAT
Conductor current	83 kA	68 kA
Operation temperature	5 K	5 K
Design stress	800 MPa	670 MPa
Weight of TF coils	11 800 tonne	5362 tonne

and stress acting in the coils, Nb_3Al was originally the prime conductor option due to its less susceptibility of the operation current to a strain. However, Fig. 9 shows that a difference in B_{max} between Nb_3Sn and Nb_3Al becomes small and that the difference is smaller than 0.3 T for $R_p \geq 8\text{ m}$. Considering this result and the technical maturity of Nb_3Sn , JA DEMO has adopted Nb_3Sn as the prime superconductor (SC) option.³⁵ A cryogenic steel qualified for the DEMO TF coil structure with $S_m = 800\text{ MPa}$ needs to show S_y of well above 1200 MPa since $S_m = 2S_y/3$, where S_y represents the 0.2% yield strength. Unfortunately, existing cryogenic steels such as JJ1 (Ref. 36) do not sufficiently satisfy the requirement. Under the circumstances, Japan plans to explore more strengthened cryogenic steels for DEMO. The leading development plan for the cryogenic steels is to optimize N and V content in existing steels such as JN1, SUS317J2, and XM-19.

VII. REMOTE MAINTENANCE

Obviously, RM is a major technical challenge in DEMO. Under the extremely high radiation environment, one has to periodically replace IVCs with remote handling (RH) equipment. In addition, the reliability and time required for the replacement will offer a key test of measuring the future potential of a fusion power plant. From the point of view of reactor design, the RM scheme is closely coupled with tokamak architecture in that it provides boundary conditions on the segmentation of IVCs, port size and port arrangement, and SC coil arrangement, etc. On a conceptual design level, various RM schemes can be planned, and actually, a lot of concepts have been assessed.

When Japan worked on compact reactor concepts, sector transport maintenance was the prime option.^{37,38} The distinctive advantages of sector transport are a reduced number of cutting and rewelding points and poloidal ring structure resisting electromagnetic and thermal deformations. The scheme seems to be attractive when the reactor size is small. However, when R_p increases up to 8 m or larger, the problem of how to transport gigantic and massive sectors safely becomes critical. In the JA DEMO, a banana segment and divertor cassette maintenance scheme were selected as a result of considerations of a variety of RM concepts.^{39–42} The tentative foreseen replacement frequency of BB segments and divertor cassettes is about 4 to 5 years and 1 to 2 years, respectively. Part of divertor heat sink is composed of Cu-alloy cooling pipe with tungsten monoblock armor.¹⁷ The radiation damage of Cu-alloy will require the frequent replacement of divertor cassettes, compared with BB segments made of RAFM steel.

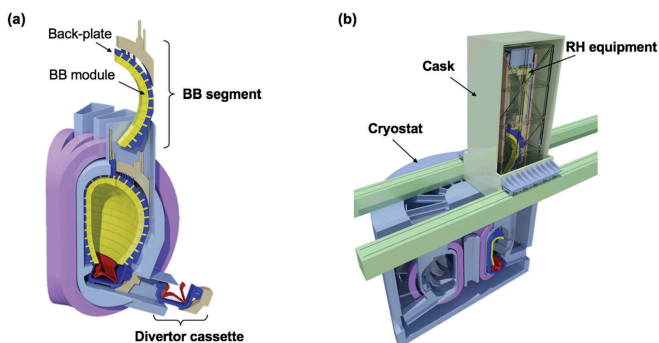


Fig. 11. (a) IVCs (BB segment and divertor cassette) removed in periodic replacement, and (b) RH equipment to transport the BB segment.

The latest RM concept is depicted in Fig. 11. The BB segment and divertor cassette are removed from the vertical and lower port located between every neighboring TF coil, respectively. The removal and transport of the BB segment requires relatively complex movements for RH equipment. The recent design on RM is devoted to a detailed design of RH equipment, including component fixation and pipe connections.⁴³

VIII. STORAGE OF RADIOACTIVE MATERIALS

The periodic replacement of IVCs anticipated in DEMO generates a large amount of radioactive materials. In the JA DEMO, BB modules and divertor cassettes are replaced every several years and every few years, respectively. All these IVCs are highly activated radioactive materials at least in 10 to 20 years after unloading from the reactor, and they need to be cooled down in temporal storage before disassembling. Figure 12 shows the contact dose rate of the IVCs after shutdown of operation, indicating that the dose rate of BB is as high as 100 and 10 Gy/h at 6 and 16 years after operation shutdown.⁴⁴ Assuming that RH equipment is operative at the dose rate of the order of 10 Gy/h or lower, the used BBs need to be cooled down for about 10 years in temporal storage. The initial assessment of temporal storage was as huge as 38 200 m² to store four full sets of the used BB segments on a safety-side design when the used BB segments are grouped into 22.5-deg assemblies to keep the assemblies in rows with gamma-ray shielding on lateral sides. Since the assessment, the waste management

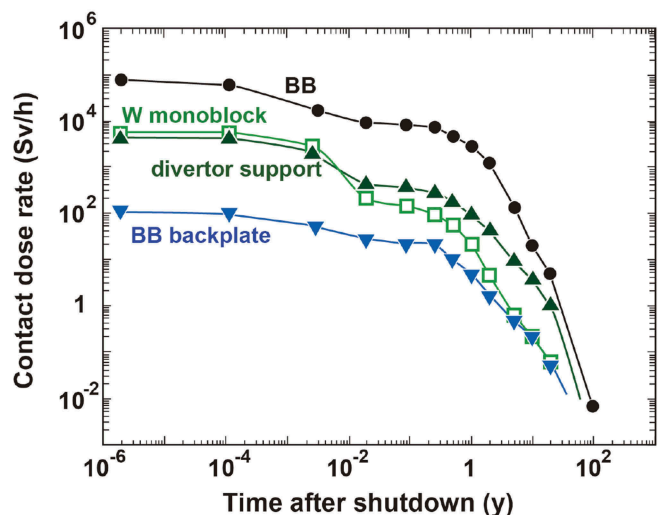


Fig. 12. Contact dose rate after operation shutdown.

strategy for downsizing the waste storage has been recognized as a challenge for DEMO.

A clue to downsizing the waste storage was proposed in Ref. 45. The idea is to store the used BB segments as they were in the VV where highly activated BB modules are arranged opposite each other around the central axis of the torus and the BB back plates play the role of radiation shield as well as BB support structure. The updated design based on the concept is shown in Fig. 13, where the used BB segments are arranged in the torus, dramatically reducing the area to 14 950 m² corresponding to 40% of the original design. In the latest design, residual heat concentrated in the

core is removed by forced cooling. The total residual heat for such a torus assembly is 2, 0.5, and 0.1 MW in 1 month, 1 year, and 4.5 years after shutdown, respectively. Figure 14 is a cut-away view of the tokamak building including waste-related facilities. Temporal storage for the used BB segments, temporal storage for the divertor cassettes, and interim waste storage for disposal are located in different floors to intensively arrange these waste-related facilities.

IX. SUMMARY

The design evolution on the JA DEMO during the past decade is outlined in this paper to characterize Japan's approach to critical DEMO design issues. The policy change of a DEMO target to lower power had a large impact on the DEMO conceptual design study during the past decade, leading to design changes in various aspects. Some of the changes are consequences of vigorous efforts to resolve puzzling design issues. The changes are summarized as follows:

1. The latest results of the conceptual design study throughout the evolution are summarized as the following: (1) baseline divertor concept is conventional SND with a divertor leg longer than ITER, (2) plasma detachment with impurity seeding, and (3) ITER-like tungsten monoblock heat sink cooled by pressurized water. The recent divertor simulation with the SONIC code indicates that the design requirement for the concept of $q_{div}^{peak} < 10 \text{ MW/m}^2$ can be attained at $f_{rad} \sim 80\%$ and $n_{sep} \sim 2 \times 10^{19} \text{ m}^{-3}$ or higher for the JA DEMO with $P_{fus} = 1.5 \text{ to } 2 \text{ GW}$.

2. The recent BB design based on the WCSB concept focuses on a simplified internal structure and pressure tightness against in-box LOCA. The full mixture of beryllide (Be_{12}V or Be_{13}Zr) and Li_2TiO_3 pebbles inside

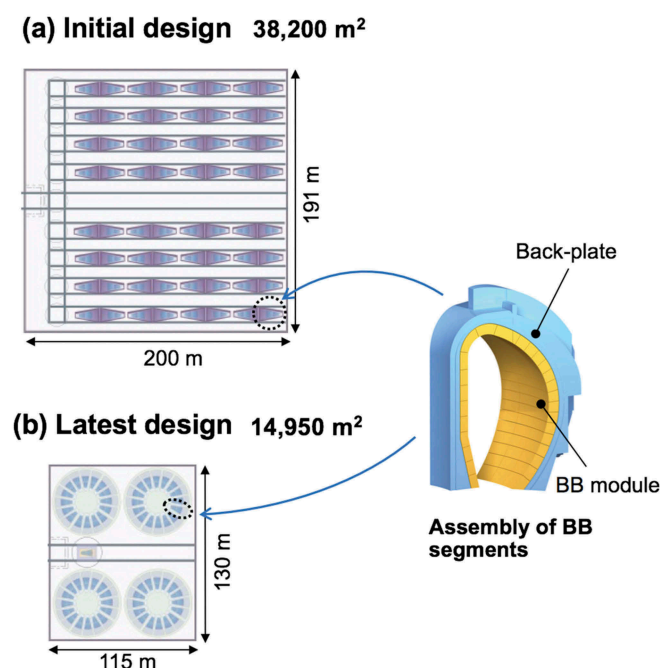


Fig. 13. Arrangement of the used BB segments for temporal waste storage: (a) initial design and (b) latest design.

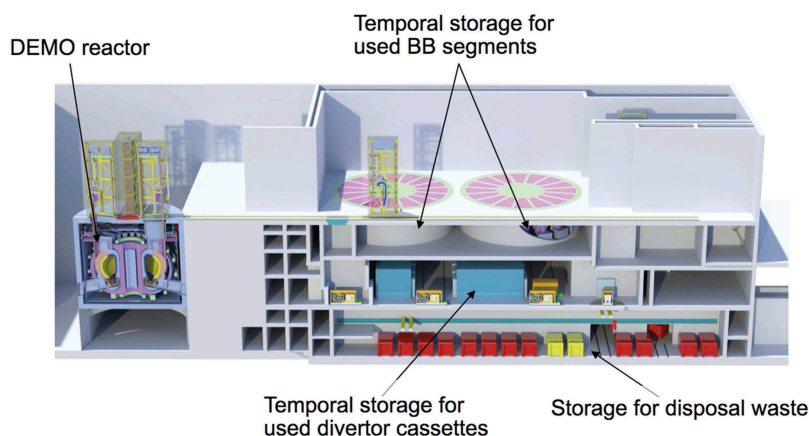


Fig. 14. Cut-away view of waste-related facilities.

the BB casing with rib structure can satisfy these requirements, albeit with a marginal TBR for self-sufficient fuel production.

3. The prime SC option of TF coils is Nb₃Sn. A critical requirement for the TF coil design is design stress which is determined to be 800 MPa, and which is larger than ITER ($S_m = 667$ 2As as a result of considerations of a variety of RM concepts, the JA DEMO has adopted a banana segment and divertor cassette maintenance scheme using vertical and lower maintenance ports. The RM scheme has a lot of technical challenges to be resolved especially in RH equipment.

4. The radioactive IVCs generated from periodic replacement need to be cooled down in temporal storage before disassembling. Downsizing temporal storage will be a significant issue in the design of the waste-related facility. The arrangement of the used BB segments in the torus dramatically reduces the area of temporal storage.

Acknowledgments

This work was carried out in the framework of the activity of the Joint Special Design Team for Fusion DEMO and partly by the DEMO Design Activity under the Broader Approach (BA). We would like to express cordial gratitude to experts of Institutes for Quantum and Radiological Science and Technology (QST), National Institute for Fusion Science (NIFS), universities, and manufacturing companies for their valuable advice and helpful support to the Special Design Team. The authors also acknowledge members of the EUROfusion PPPT Team for stimulating discussion in BA DEMO design activities. This work was partly supported by KAKENHI Grant-in-Aid for Scientific Research (C), No. 17K07002.

References

1. G. FEDERICI et al., "Overview of EU DEMO Design and R&D Activities," *Fusion Eng. Des.*, **89**, 882 (2014); <https://doi.org/10.1016/j.fusengdes.2014.01.070>.
2. Y. T. SONG et al., "Concept Design of CFETR Tokamak Machine," *IEEE Trans. Plasma Sci.*, **42**, 503 (2014); <https://doi.org/10.1109/TPS.2014.2299277>.
3. C. E. KESSEL et al., "The Fusion Nuclear Science Facility, the Critical Step in the Pathway to Fusion Energy," *Fusion Sci. Technol.*, **68**, 225 (2014); <https://doi.org/10.13182/FST14-953>.
4. A. M. GOROFALO et al., "A Fusion Neutron Science Facility for a Fast-Track Path to DEMO," *Fusion Eng. Des.*, **89**, 876 (2014); <https://doi.org/10.1016/j.fusengdes.2014.03.055>.
5. K. KIM et al., "Design Concept of K-DEMO for Near-Term Implementation," *Nucl. Fusion*, **55**, 053027 (2015); <https://doi.org/10.1088/0029-5515/55/5/053027>.
6. B. V. KUTEEV et al., "Intense Fusion Neutron Sources," *Plasma Phys. Rep.*, **36**, 281 (2010); <https://doi.org/10.1134/S1063780X1004001X>.
7. K. TOBITA et al., "Design Study of Fusion DEMO Plant at JAERI," *Fusion Eng. Des.*, **81**, 1151 (2006); <https://doi.org/10.1016/j.fusengdes.2005.08.058>.
8. K. TOBITA et al., "SlimCS—Compact Low Aspect Ratio DEMO Reactor with Reduced-Size Central Solenoid," *Nucl. Fusion*, **47**, 829 (2007); <https://doi.org/10.1088/0029-5515/47/8/022>.
9. R. HIWATARI et al., "Demonstration Tokamak Fusion Power Plant for Early Realization of Net Electric Power Generation," *Nucl. Fusion*, **45**, 96 (2005); <https://doi.org/10.1088/0029-5515/45/2/004>.
10. R. HIWATARI et al., "Analysis of Critical Development Issues Towards Advanced Tokamak Power Plant CREST," *Nucl. Fusion*, **45**, 387 (2007); <https://doi.org/10.1088/0029-5515/47/5/003>.
11. "National Policy of Future Nuclear Fusion Research and Development", Atomic Energy Commission, Advisory Committee on Nuclear Fusion (2005); http://www.aec.go.jp/jicst/NC/senmon/kakuyugo2/siryu/kettei/houkoku051026_e/index.htm (current as of June 15, 2018).
12. H. YAMADA et al., "Japanese Endeavors to Establish Technological Bases for DEMO," *Fusion Eng. Des.*, **109–111**, 1318 (2016); <https://doi.org/10.1016/j.fusengdes.2015.12.035>.
13. K. TOBITA et al., "Design Strategy and Recent Design Activity on Japan's DEMO," *Fusion Sci. Technol.*, **72**, 537 (2017); <https://doi.org/10.1080/15361055.2017.1364112>.
14. "A Roadmap Toward Fusion DEMO Reactor (First Report)," Science and Technology Committee on Fusion Energy (2018); http://www.mext.go.jp/component/b_menu/shingi/toushin/_icsFiles/afieldfile/2018/11/08/1408259_2_1_1.pdf (current as of June 15, 2018).
15. Y. SAKAMOTO et al., "DEMO Concept Development and Assessment of Relevant Technologies," IAEA 25th Fusion Energy Conf., FIR/3-4Rb, St. Petersburg, Russia, October 13-18, 2014; http://www.naweb.iaea.org/naweb/physics/FEC/FEC2014/fec2014-preprints/222_FIP34Rb.pdf (current as of June 15, 2018).
16. Y. MIYOSHI et al., "Cooling Water System Design of Japan's DEMO for Fusion Power Production," *Fusion Eng. Des.*, **126**, 110 (2018); <https://doi.org/10.1016/j.fusengdes.2017.11.013>.
17. N. ASAKURA et al., "Studies of Power Exhaust and Divertor Design for a 1.5 GW-Level Fusion Power DEMO," *Nucl. Fusion*, **57**, 126050 (2017); <https://doi.org/10.1088/1741-4326/aa867a>.
18. N. ASAKURA et al., "Simulation Study of Power Load with Impurity Seeding in Advanced Divertor 'Short Super-X

- Divertor' for a Tokamak Reactor," *J. Nucl. Mater.*, **463**, 1238 (2015); <https://doi.org/10.1016/j.jnucmat.2015.01.068>.
19. K. TOBITA, G. FEDERICI, and K. OKANO, "Research and Development Status on Fusion DEMO Reactor Design Under Broader Approach," *Fusion Eng. Des.*, **89**, 1780 (2014); <https://doi.org/10.1016/j.fusengdes.2014.02.077>.
 20. N. ASAKURA et al., "Plasma Exhaust and Divertor Studies in Japan and Europe Broader Approach, DEMO Design Activity," *Fusion Eng. Des.*, **136**, 1214 (2018); <https://doi.org/10.1016/j.fusengdes.2018.04.104>.
 21. N. ASAKURA et al., "A Simulation Study of Large Power Handling in the Divertor for A DEMO Reactor," *Nucl. Fusion*, **53**, 123013 (2013); <https://doi.org/10.1088/0029-5515/53/12/123013>.
 22. K. HOSHINO et al., "Progress of Divertor Study on DEMO Design," *Plasma Fusion Res.*, **12**, 140502 (2017); <https://doi.org/10.1585/pfr.12.1405023>.
 23. K. HOSHINO et al., "Photon Trapping Effects in DEMO Divertor Plasma," *Contrib. Plasma Phys.*, **56**, 657 (2016); <https://doi.org/10.1002/ctpp.201610039>.
 24. K. HOSHINO et al., "Multi-Impurity Divertor Simulation Using a Monte Carlo Kinetic Impurity Transport Model," *Contrib. Plasma Phys.*, **58**, 638 (2018); <https://doi.org/10.1002/ctpp.201700166>.
 25. Y. SAKAMOTO et al., "Development of Physics and Engineering Designs for Japan's DEMO Concept," IAEA 27th Fusion Energy Conf., FIP/3-2, Gandhinagar, India, October 22-27, 2018.
 26. K. TOBITA et al., "Search for Reality of Solid Breeder Blanket for DEMO," *Fusion Eng. Des.*, **85**, 1342 (2010); <https://doi.org/10.1016/j.fusengdes.2010.03.038>.
 27. M. ENOEDA et al., "Design and Technology Development of Solid Breeder Blanket Cooled by Supercritical Water in Japan," *Nucl. Fusion*, **43**, 1837 (2003); <https://doi.org/10.1088/0029-5515/43/12/026>.
 28. Y. SOMEYA et al., "Simplification of Blanket System for SlimCS Fusion DEMO Reactor," *Fusion Eng. Des.*, **86**, 2268 (2011); <https://doi.org/10.1016/j.fusengdes.2011.01.141>.
 29. Y. SOMEYA et al., "Development of Water-Cooled Blanket Concept with Pressure Tightness Against In-Box LOCA for JA DEMO," *Fusion Eng. Des.* (in press 2019); <https://doi.org/10.1016/j.fusengdes.2019.01.107>.
 30. M. NAKAMICHI et al., "Elementary Development for Beryllide Pebble Fabrication by Rotating Electrode Method," *Fusion Eng. Des.*, **69**, 491 (2003); [https://doi.org/10.1016/S0920-3796\(03\)00394-6](https://doi.org/10.1016/S0920-3796(03)00394-6).
 31. M. NAKAMICHI and J.-H. KIM, "Homogenization Treatment to Stabilize the Compositional Structure of Beryllide Pebbles," *J. Nucl. Mater.*, **440**, 530 (2013); <https://doi.org/10.1016/j.jnucmat.2013.02.070>.
 32. M. NAKAMICHI, J.-H. KIM, and P. KURINSKIY, "Characterization of Vanadium Beryllide Pebble Bed for the Japan DEMO Blanket Application," *Fusion Eng. Des.*, **136**, 125 (2018); <https://doi.org/10.1016/j.fusengdes.2018.01.022>.
 33. J.-H. KIM and M. NAKAMICHI, "Anomalous Oxidation Behavior in a Zirconium Beryllium Intermetallic Compound," *J. Nucl. Mater.*, **519**, 182 (2019); <https://doi.org/10.1016/j.jnucmat.2019.03.042>.
 34. H. UTOH et al., "SCONE Code: Superconducting TF Coils Design Code for Tokamak Fusion Reactor," *J. Plasma Fusion Res. Ser.*, **9**, 304 (2010).
 35. K. TOBITA et al., "Conceptual Design of Japan's Fusion DEMO Reactor, (JA DEMO), and Superconducting Coil Issues," *J. Phys.: Conference Series* (accepted for publication).
 36. K. HAMADA et al., "Demonstration of Full Scale JJ1 and 316LN Fabrication for ITER TF Coil Structure," *Fusion Eng. Des.*, **82**, 1481 (2007); <https://doi.org/10.1016/j.fusengdes.2007.07.032>.
 37. K. TOBITA et al., "Maintenance Concept for the SlimCS DEMO Reactor," *Fusion Eng. Des.*, **86**, 2730 (2011); <https://doi.org/10.1016/j.fusengdes.2011.03.022>.
 38. H. UTOH et al., "Conceptual Study of Vertical Sector Transport Maintenance for DEMO Fusion Reactor," *Fusion Eng. Des.*, **88**, 1409 (2012); <https://doi.org/10.1016/j.fusengdes.2012.03.024>.
 39. H. UTOH et al., "Evaluation of Remote Maintenance Schemes by Plasma Equilibrium Analysis in Tokamak DEMO Reactor," *Fusion Eng. Des.*, **89**, 2588 (2014); <https://doi.org/10.1016/j.fusengdes.2014.06.020>.
 40. H. UTOH et al., "Comparative Evaluation of Remote Maintenance Schemes for Fusion DEMO Reactor," *Fusion Eng. Des.*, **98–99**, 1648 (2015); <https://doi.org/10.1016/j.fusengdes.2015.06.139>.
 41. H. UTOH et al., "Design Concept of Conducting Shell and In-Vessel Components Stable for Plasma Vertical Stability and Remote Maintenance Scheme in Fusion DEMO," *Fusion Eng. Des.*, **103**, 93 (2016); <https://doi.org/10.1016/j.fusengdes.2015.12.048>.
 42. H. UTOH et al., "Technological Assessments Between Vertical and Horizontal Remote Maintenance Schemes for DEMO Reactor," *Fusion Eng. Des.*, **124**, 596 (2017); <https://doi.org/10.1016/j.fusengdes.2017.03.036>.
 43. K. TOBITA et al., "Overview of the DEMO Conceptual Design Activity in Japan," *Fusion Eng. Des.*, **136**, 1024 (2018); <https://doi.org/10.1016/j.fusengdes.2018.04.059>.
 44. Y. SOMEYA et al., "Management Strategy for Radioactive Waste in the Fusion DEMO Reactor," *Fusion Sci. Technol.*, **68**, 423 (2015); <https://doi.org/10.13182/FST15-101>.
 45. M. KONDO et al., "Conceptual Design of Temporally Storage Area in Hot Cell for Fusion DEMO Reactor," *Plasma Fusion Res.*, **11**, 2405077 (2016); <https://doi.org/10.1585/pfr.11.2405077>.